EUROPEAN ORGANISATION FOR NUCLEAR RESEARCH

CERN PPE/96-140
14 October.1996

Search for Unstable Neutral and Charged Heavy Leptons in e^+e^- Collisions at $\sqrt{s} = 161$ GeV

The OPAL Collaboration

Abstract

Searches for unstable neutral and charged heavy leptons (L^0, $L^\pm$) have been performed using a data sample of 10.0 pb^{-1} at a centre-of-mass energy of $\sqrt{s}$ = 161.3 GeV collected with the OPAL detector at LEP during July and August 1996. Two candidate events were observed after the selection, which is consistent with the expected total background of 1.57 events, and lower limits have been derived on heavy lepton masses for various models. If an unstable Dirac neutral heavy lepton, L^0, decays only into eW^*, μW^* or τW^*, the lower limits on its mass at the 95% C.L. are 69.3 GeV, 72.0 GeV and 66.0 GeV, respectively. The limits are modified for a Majorana L^0 to 59.5 GeV, 60.5 GeV and 55.7 GeV, respectively. If an unstable heavy charged lepton, $L^\pm$, decays into a stable heavy neutrino, and if $m_{L^\pm} - m_{\nu_L} > 13$ GeV, a lower limit on its mass of 73.5 GeV is obtained. If the $L^\pm$ decays through lepton flavour mixing into a massless neutrino ν_ℓ and $W^{*\pm}$, the lower limit on $m_{L^\pm}$ was determined to be 76.7 GeV at 95% C.L.

To be submitted to Physics Letters B

The OPAL Collaboration

K. Ackerstaff[8], G. Alexander[23], J. Allison[16], N. Altekamp[5], K. Ametewee[25], K.J. Anderson[9], S. Anderson[12], S. Arcelli[2], S. Asai[24], D. Axen[29], G. Azuelos[18,a], A.H. Ball[17], E. Barberio[8], R.J. Barlow[16], R. Bartoldus[3], J.R. Batley[5], J. Bechtluft[14], C. Beeston[16], T. Behnke[8], A.N. Bell[1], K.W. Bell[20], G. Bella[23], S. Bentvelsen[8], P. Berlich[10], S. Bethke[14], O. Biebel[14], V. Blobel[27], I.J. Bloodworth[1], J.E. Bloomer[1], M. Bobinski[10], P. Bock[11], H.M. Bosch[11], M. Boutemeur[34], B.T. Bouwens[12], S. Braibant[12], R.M. Brown[20], H.J. Burckhart[8], C. Burgard[8], R. Bürgin[10], P. Capiluppi[2], R.K. Carnegie[6], A.A. Carter[13], J.R. Carter[5], C.Y. Chang[17], D.G. Charlton[1,b], D. Chrisman[4], P.E.L. Clarke[15], I. Cohen[23], J.E. Conboy[15], O.C. Cooke[16], M. Cuffiani[2], S. Dado[22], C. Dallapiccola[17], G.M. Dallavalle[2], S. De Jong[12], L.A. del Pozo[8], K. Desch[3], M.S. Dixit[7], E. do Couto e Silva[12], M. Doucet[18], E. Duchovni[26], G. Duckeck[34], I.P. Duerdoth[16], J.E.G. Edwards[16], P.G. Estabrooks[6], H.G. Evans[9], M. Evans[13], F. Fabbri[2], P. Fath[11], F. Fiedler[27], M. Fierro[2], H.M. Fischer[3], R. Folman[26], D.G. Fong[17], M. Foucher[17], A. Fürtjes[8], P. Gagnon[7], J.W. Gary[4], J. Gascon[18], S.M. Gascon-Shotkin[17], N.I. Geddes[20], C. Geich-Gimbel[3], T. Geralis[20], G. Giacomelli[2], P. Giacomelli[4], R. Giacomelli[2], V. Gibson[5], W.R. Gibson[13], D.M. Gingrich[30,a], D. Glenzinski[9], J. Goldberg[22], M.J. Goodrick[5], W. Gorn[4], C. Grandi[2], E. Gross[26], J. Grunhaus[23] M. Gruwé[8], C. Hajdu[32], G.G. Hanson[12], M. Hansroul[8], M. Hapke[13], C.K. Hargrove[7], P.A. Hart[9], C. Hartmann[3], M. Hauschild[8], C.M. Hawkes[5], R. Hawkings[8], R.J. Hemingway[6], M. Herndon[17], G. Herten[10], R.D. Heuer[8], M.D. Hildreth[8], J.C. Hill[5], S.J. Hillier[1], T. Hilse[10], P.R. Hobson[25], R.J. Homer[1], A.K. Honma[28,a], D. Horváth[32,c], R. Howard[29], R.E. Hughes-Jones[16], D.E. Hutchcroft[5], P. Igo-Kemenes[11], D.C. Imrie[25], M.R. Ingram[16], K. Ishii[24], A. Jawahery[17], P.W. Jeffreys[20], H. Jeremie[18], M. Jimack[1], A. Joly[18], C.R. Jones[5], G. Jones[16], M. Jones[6], R.W.L. Jones[8], U. Jost[11], P. Jovanovic[1], T.R. Junk[8], D. Karlen[6], K. Kawagoe[24], T. Kawamoto[24], R.K. Keeler[28], R.G. Kellogg[17], B.W. Kennedy[20], B.J. King[8], J. Kirk[29], S. Kluth[8], T. Kobayashi[24], M. Kobel[10], D.S. Koetke[6], T.P. Kokott[3], M. Kolrep[10], S. Komamiya[24], T. Kress[11], P. Krieger[6], J. von Krogh[11], P. Kyberd[13], G.D. Lafferty[16], R. Lahmann[17], W.P. Lai[19], D. Lanske[14], J. Lauber[15], S.R. Lautenschlager[31], J.G. Layter[4], D. Lazic[22], A.M. Lee[31], E. Lefebvre[18], D. Lellouch[26], J. Letts[2], L. Levinson[26], C. Lewis[15], S.L. Lloyd[13], F.K. Loebinger[16], G.D. Long[17], M.J. Losty[7], J. Ludwig[10], M. Mannelli[8], S. Marcellini[2], C. Markus[3], A.J. Martin[13], J.P. Martin[18], G. Martinez[17], T. Mashimo[24], W. Matthews[25], P. Mättig[3], W.J. McDonald[30], J. McKenna[29], E.A. Mckigney[15], T.J. McMahon[1], A.I. McNab[13], R.A. McPherson[8], F. Meijers[8], S. Menke[3], F.S. Merritt[9], H. Mes[7], J. Meyer[27], A. Michelini[2], G. Mikenberg[26], D.J. Miller[15], R. Mir[26], W. Mohr[10], A. Montanari[2], T. Mori[24], M. Morii[24], U. Müller[3], K. Nagai[26], I. Nakamura[24], H.A. Neal[8], B. Nellen[3], B. Nijjhar[16], R. Nisius[8], S.W. O'Neale[1], F.G. Oakham[7], F. Odorici[2], H.O. Ogren[12], N.J. Oldershaw[16], T. Omori[24], M.J. Oreglia[9], S. Orito[24], J. Pálinkás[33,d], G. Pásztor[32], J.R. Pater[16], G.N. Patrick[20], J. Patt[10], M.J. Pearce[1], S. Petzold[27], P. Pfeifenschneider[14], J.E. Pilcher[9], J. Pinfold[30], D.E. Plane[8], P. Poffenberger[28], B. Poli[2], A. Posthaus[3], H. Przysiezniak[30], D.L. Rees[1], D. Rigby[1], S. Robertson[28], S.A. Robins[13], N. Rodning[30], J.M. Roney[28], A. Rooke[15], E. Ros[8], A.M. Rossi[2], M. Rosvick[28], P. Routenburg[30], Y. Rozen[22], K. Runge[10], O. Runolfsson[8], U. Ruppel[14], D.R. Rust[12], R. Rylko[25], K. Sachs[10], E.K.G. Sarkisyan[23], M. Sasaki[24], C. Sbarra[2], A.D. Schaile[34], O. Schaile[34], F. Scharf[3], P. Scharff-Hansen[8], P. Schenk[27], B. Schmitt[8], S. Schmitt[11], M. Schröder[8], H.C. Schultz-Coulon[10], M. Schulz[8], M. Schumacher[3], P. Schütz[3], W.G. Scott[20], T.G. Shears[16], B.C. Shen[4], C.H. Shepherd-Themistocleous[8], P. Sherwood[15], G.P. Siroli[2], A. Sittler[27],

A. Skillman[15], A. Skuja[17], A.M. Smith[8], T.J. Smith[28], G.A. Snow[17], R. Sobie[28], S. Söldner-Rembold[10], R.W. Springer[30], M. Sproston[20], A. Stahl[3], M. Steiert[11], K. Stephens[16], J. Steuerer[27], B. Stockhausen[3], D. Strom[19], F. Strumia[8], P. Szymanski[20], R. Tafirout[18], S.D. Talbot[1], S. Tanaka[24], P. Taras[18], S. Tarem[22], M. Thiergen[10], M.A. Thomson[8], E. von Törne[3], S. Towers[6], I. Trigger[18], T. Tsukamoto[24], E. Tsur[23], A.S. Turcot[9], M.F. Turner-Watson[8], P. Utzat[11], R. Van Kooten[12], M. Verzocchi[10], P. Vikas[18], M. Vincter[28], E.H. Vokurka[16], F. Wäckerle[10], A. Wagner[27], C.P. Ward[5], D.R. Ward[5], J.J. Ward[15], P.M. Watkins[1], A.T. Watson[1], N.K. Watson[7], P.S. Wells[8], N. Wermes[3], J.S. White[28], B. Wilkens[10], G.W. Wilson[27], J.A. Wilson[1], G. Wolf[26], S. Wotton[5], T.R. Wyatt[16], S. Yamashita[24], G. Yekutieli[26], V. Zacek[18],

[1]School of Physics and Space Research, University of Birmingham, Birmingham B15 2TT, UK
[2]Dipartimento di Fisica dell' Università di Bologna and INFN, I-40126 Bologna, Italy
[3]Physikalisches Institut, Universität Bonn, D-53115 Bonn, Germany
[4]Department of Physics, University of California, Riverside CA 92521, USA
[5]Cavendish Laboratory, Cambridge CB3 0HE, UK
[6] Ottawa-Carleton Institute for Physics, Department of Physics, Carleton University, Ottawa, Ontario K1S 5B6, Canada
[7]Centre for Research in Particle Physics, Carleton University, Ottawa, Ontario K1S 5B6, Canada
[8]CERN, European Organisation for Particle Physics, CH-1211 Geneva 23, Switzerland
[9]Enrico Fermi Institute and Department of Physics, University of Chicago, Chicago IL 60637, USA
[10]Fakultät für Physik, Albert Ludwigs Universität, D-79104 Freiburg, Germany
[11]Physikalisches Institut, Universität Heidelberg, D-69120 Heidelberg, Germany
[12]Indiana University, Department of Physics, Swain Hall West 117, Bloomington IN 47405, USA
[13]Queen Mary and Westfield College, University of London, London E1 4NS, UK
[14]Technische Hochschule Aachen, III Physikalisches Institut, Sommerfeldstrasse 26-28, D-52056 Aachen, Germany
[15]University College London, London WC1E 6BT, UK
[16]Department of Physics, Schuster Laboratory, The University, Manchester M13 9PL, UK
[17]Department of Physics, University of Maryland, College Park, MD 20742, USA
[18]Laboratoire de Physique Nucléaire, Université de Montréal, Montréal, Quebec H3C 3J7, Canada
[19]University of Oregon, Department of Physics, Eugene OR 97403, USA
[20]Rutherford Appleton Laboratory, Chilton, Didcot, Oxfordshire OX11 0QX, UK
[22]Department of Physics, Technion-Israel Institute of Technology, Haifa 32000, Israel
[23]Department of Physics and Astronomy, Tel Aviv University, Tel Aviv 69978, Israel
[24]International Centre for Elementary Particle Physics and Department of Physics, University of Tokyo, Tokyo 113, and Kobe University, Kobe 657, Japan
[25]Brunel University, Uxbridge, Middlesex UB8 3PH, UK
[26]Particle Physics Department, Weizmann Institute of Science, Rehovot 76100, Israel
[27]Universität Hamburg/DESY, II Institut für Experimental Physik, Notkestrasse 85, D-22607 Hamburg, Germany
[28]University of Victoria, Department of Physics, P O Box 3055, Victoria BC V8W 3P6, Canada

[29]University of British Columbia, Department of Physics, Vancouver BC V6T 1Z1, Canada
[30]University of Alberta, Department of Physics, Edmonton AB T6G 2J1, Canada
[31]Duke University, Dept of Physics, Durham, NC 27708-0305, USA
[32]Research Institute for Particle and Nuclear Physics, H-1525 Budapest, P O Box 49, Hungary
[33]Institute of Nuclear Research, H-4001 Debrecen, P O Box 51, Hungary
[34]Ludwigs-Maximilians-Universität München, Sektion Physik, Am Coulombwall 1, D-85748 Garching, Germany

[a] and at TRIUMF, Vancouver, Canada V6T 2A3
[b] and Royal Society University Research Fellow
[c] and Institute of Nuclear Research, Debrecen, Hungary
[d] and Department of Experimental Physics, Lajos Kossuth University, Debrecen, Hungary

1 Introduction

This paper presents searches for pair production of unstable neutral heavy leptons $L^0\bar{L}^0$ and unstable charged heavy leptons L^+L^- in e^+e^- collisions[1]. The data used in this analysis correspond to an integrated luminosity of 10.0 pb^{-1} at a centre-of-mass energy of $\sqrt{s}$ = 161.3 GeV collected with the OPAL detector at LEP during July and August 1996.

The precise measurements of the Z boson parameters by the LEP1 ($\sqrt{s} \sim M_Z$) and SLC experiments have determined the number of species of light neutrinos to be three [1]. However, this does not exclude a fourth generation in which all the fermions are heavy. Lower limits on the masses of heavy leptons were obtained at LEP1 [1, 2] and recent searches at LEP1.5, ($\sqrt{s}$ = 130 and 136 GeV), have improved the limits [3, 4].

Neutral heavy lepton pairs $L^0\bar{L}^0$ could be produced in e^+e^- annihilation via a virtual Z^0 boson and its cross-section is given in Ref. [5]. The following decay mode was considered for L^0:

(A) $L^0 \to \ell W^*$ via lepton flavour mixing, where ℓ is e, μ or τ, and W^* is a virtual W boson.

A Majorana L^0 can decay into either $\ell^- W^{*+}$ or $\ell^+ W^{*-}$. Therefore, in order to be sensitive to both Dirac and Majorana L^0, charged correlation between the two light leptons was not used in the analysis. The 95% C.L. lower mass limit at LEP1.5 for an unstable L^0 was 63.0 GeV for a Dirac L^0 and 54.3 GeV for a Majorana L^0, assuming the coupling for $L^0L^0Z^*$ is the same as for $\nu_\ell\nu_\ell Z^*$ [3, 4]. The visible energy of these events is expected to be large and there should be at least four charged particles, including at least two light leptons (e, μ or τ), in an event.

Charged heavy lepton pairs L^+L^- could be produced in e^+e^- annihilation via a virtual Z^0 boson or a virtual photon. The cross-section for L^+L^- production is given in Ref. [5]. The following two cases were studied for the decay of L^-:

(B) $L^- \to \nu_L W^{*-}$, where ν_L is a stable heavy neutrino. The lower mass limit based on data from LEP1 for the heavy stable neutrino (ν_L) was 45.0 GeV for a Dirac neutrino and 39.5 GeV for a Majorana neutrino [1, 2]. In this analysis, the ν_L is therefore assumed to be heavier than 39.5 GeV. On the same assumption the searches at LEP1.5 [3, 4] set the lower limit on the mass of the L^- at 64.5 GeV, if $m_{L^\pm} - m_{\nu_L} > 10$ GeV.

(C) $L^- \to \nu_\ell W^{*-}$, where ν_ℓ is ν_e, ν_μ or ν_τ. The decay occurs via lepton flavour mixing. The experimental 95% C.L. limit from LEP1.5 data was $m_{L^-} > 65.0$ GeV [3, 4].

The ordinary V–A coupling was assumed for the $L^-\nu_L W^{*-}$ and $L^-\nu_\ell W^{*-}$ decay vertices. The expected experimental signature for L^+L^- events for both cases is that of a multijet[2] event with a large unbalanced transverse momentum with respect to the beam axis. If all the visible decay products of L^- and L^+ happened to be in the same hemisphere, the event topology could be a monojet. The events in case (B) are expected to have a smaller visible energy than for case (C), because the two heavy neutrinos carry away more energy and momentum.

[1] Throughout this paper, charge conjugation is implicitly assumed. L^- denotes an unstable charged heavy lepton, L^0 denotes an unstable neutral heavy lepton and ν_L denotes a stable heavy neutrino.

[2] An isolated lepton is treated as a jet.

Cascade decays ($L^0 \to L^- \to \nu_\ell$ and $L^- \to L^0 \to \ell$) of heavy leptons were not considered in this analysis. The analysis was designed to have a good sensitivity for heavy leptons with a decay length shorter than a few cm. Namely, the mixing parameters of L^0–ℓ^- and L^-–ν_ℓ were assumed to satisfy the condition $\sum_\ell |V_{L^0\ell}|^2 > \mathcal{O}(10^{-12})$ for case (A) and $\sum_\ell |V_{L^-\nu_\ell}|^2 > \mathcal{O}(10^{-12})$ for case (C), where $V_{L^0\ell}$ is the flavour mixing parameter between a neutral heavy lepton and a light lepton (e, μ or τ) and $V_{L^-\nu_\ell}$ is the flavour mixing parameter between a charged heavy lepton and a light neutrino (ν_e, ν_μ or ν_τ).

The two W^* bosons in an $L^0\bar{L}^0$ or L^+L^- event can decay either leptonically or hadronically. The analysis presented here is sensitive to all the possible combinations of the decay topologies and was designed to search for heavy leptons with masses above the current LEP experimental limits.

2 The OPAL Detector and Event Simulation

2.1 The OPAL Detector

The OPAL detector, which is described in detail in [6], is a multi-purpose apparatus having nearly complete solid angle coverage. The central detector consists of a silicon microvertex detector and a system of tracking chambers providing charged particle tracking over 96% of the full solid angle[3] inside a uniform 0.435 T magnetic field. The solenoid is surrounded by a time-of-flight (TOF) scintillating counter array. A lead-glass electromagnetic (EM) calorimeter located outside the magnet coil covers the full azimuthal range with excellent hermeticity in the polar angle range of $|\cos\theta| < 0.82$ for the barrel region and $0.81 < |\cos\theta| < 0.984$ for the endcap region. The magnet return yoke is instrumented for hadron calorimetry (HCAL), consisting of barrel and endcap sections along with pole tip detectors that together cover the region $|\cos\theta| < 0.99$. Calorimeters close to the beam axis measure the luminosity using small-angle Bhabha scattering events and complete the geometrical acceptance down to 26 mrad from the beam axis. These include the forward detectors which are lead-scintillator sandwich calorimeters and, at smaller angles, silicon tungsten calorimeters located on both sides of the interaction point. The gap between the endcap EM calorimeter and the forward detector is filled by an additional lead-scintillator electromagnetic calorimeter, called the gamma-catcher. The trigger efficiency for signal events was larger than 99.7% for all channels considered.

2.2 Monte Carlo Event Simulation

$L^0\bar{L}^0$ and L^+L^- events have been simulated by the TIPTOP [7] generator, which includes the effects of spin correlations in the weak decays. TIPTOP was modified so that JETSET 7.4 [8] could be used for the hadronization, which includes gluon radiation. Initial state photon radiation was implemented in TIPTOP based on the calculations of Berends *et al.* [9] $L^0\bar{L}^0$ events were generated at 8 values of the heavy neutral lepton mass from 45 to 80 GeV for each of the three different final states $eW^* + eW^*$, $\mu W^* + \mu W^*$ and $\tau W^* + \tau W^*$, for Majorana and Dirac

[3] A right-handed coordinate system is adopted, where the x-axis points to the centre of the LEP ring, and positive z is along the electron beam direction. The angles θ and ϕ are the polar and azimuthal angles, respectively.

cases separately. L^+L^- events were generated at 26 points in the (m_{L^-}, m_{ν_L}) plane for case (B) and at 5 mass values of heavy leptons from 60 to 80 GeV for case (C).

The following background processes were simulated in this analysis:

• The PYTHIA 5.7 [8] Monte Carlo generator was used for multihadron ($e^+e^- \to q\bar{q}(\gamma)$) events.

• $\tau^+\tau^-(\gamma)$ and $\mu^+\mu^-(\gamma)$ events were simulated by the KORALZ [10] program. The BHWIDE [11] generator was used for the $e^+e^- \to e^+e^-(\gamma)$ events.

• The PYTHIA 5.7 and PHOJET [12] Monte Carlo programs were used for generating events from two-photon processes where the Q^2 of both photons is smaller than 1.0 GeV^2 and the invariant mass of the photon-photon system ($M^2_{\gamma\gamma}$) is greater than 4 GeV^2. For events with higher Q^2 the generators PYTHIA 5.7 and HERWIG [13] were used. Four-lepton events were simulated by the Vermaseren generator [14]. Event samples for all the possible processes (final state hadrons from point-like $\gamma\gamma \to q\bar{q}$ processes and from vector meson dominance, and all $e^+e^-\ell^+\ell^-$ final states) were generated. Two-photon events were not generated in the region where $Q^2 < 1.0$ GeV^2 and $M^2_{\gamma\gamma} < 4$ GeV^2, or $Q^2 > 1.0$ GeV^2 and $M^2_{\gamma\gamma} < 3$ GeV^2. This region did not represent a serious background to the search presented here.

• Events from four-fermion processes ($\ell^+\ell^- q\bar{q}$, $\ell^-\bar{\nu}_\ell q\bar{q}'$, $\nu_\ell\bar{\nu}_\ell q\bar{q}$, $\nu_\ell\bar{\nu}_\ell\ell^+\ell^-$), including W^+W^- events, are a serious background for the $L^0\bar{L}^0$ and L^+L^- searches. The EXCALIBUR [15] Monte Carlo program was used to simulate all four-fermion processes, including W^+W^- events. Since the event sample that we have generated using EXCALIBUR does not include $e^+e^- \to We\nu$ and $e^+e^- \to Z^*e^+e^-$ or $\gamma^*e^+e^-$ events in which one of the electrons scatters at a very low angle, these events were simulated by PYTHIA.

Generated signal and background events were processed through the full simulation of the OPAL detector [16], and the same event analysis chain was applied to these simulated events as to the data.

3 Data Analysis

Charged particle tracks were selected with similar track quality requirements as in Ref. [17]. The one change was to relax the cut on the distance of closest approach to the beam axis in the x-y plane, $|d_0|$, from 2.5 cm to 8.0 cm, recovering acceptance for long lived L^- and L^0 candidates whose decay lengths are up to 10 cm. The rest of the criteria were as follows. Tracks were required to have at least 20 measured spatial hits, more than 50% of the hits geometrically expected, and a transverse momentum exceeding 50 MeV. Electromagnetic clusters in the barrel region were required to have an energy of at least 100 MeV, and the clusters in the endcaps to have an energy of at least 250 MeV and to contain at least two adjacent lead glass blocks. Clusters in the hadron calorimeters were required to have an energy of at least 0.6 GeV in the barrel and endcaps, and at least 2 GeV in the pole tip detectors. The silicon tungsten calorimeter clusters were required to have at least 2 GeV of deposited energy. Furthermore, clusters in the forward calorimeter were required to have at least 1.5 GeV and in the gamma-catcher at least 5 GeV. Background from cosmic rays was suppressed by requiring at least one track to have a hit in the TOF counter within 10 ns of the expected time-of-flight.

Event observables such as the total visible energy or hemisphere momenta were calculated as follows. The track momenta and the momentum vectors of EM or HCAL calorimeter clusters not associated with charged tracks were first summed. When a calorimeter cluster was

associated with charged tracks, the scalar sum of the associated charged track momenta was subtracted from the cluster energy to reduce double counting. If the energy of a cluster was smaller than the scalar sum of the associated track momenta, the cluster energy was not used. The masses of all charged particles were set to the charged pion mass and the invariant masses of the energy clusters were assumed to be zero. Jets were formed using the Durham algorithm [18] with a jet resolution parameter of $y_{\rm cut} = 0.004$.

3.1 Selection of $\mathrm{L}^0\bar{\mathrm{L}}^0$ candidates (case A)

The following event selection criteria were applied. The numbers of remaining events up to and including each cut are listed in Table 1, for data and for simulated background and signal samples. The difference in the numbers of events between the data and the total simulated background at early stage (before cut (A4)) is mainly due to incomplete modelling of two-photon processes ('$\gamma\gamma$').

(A1) The number of tracks was required to be at least four, and the ratio of the number of tracks which satisfied the quality criteria to the total number of reconstructed tracks was required to be larger than 0.2 in order to reject beam-gas and beam-wall background events.

(A2) In order to reduce the background from two-photon processes and multihadronic events in which one of the jet axes was close to the beam direction, the sum of the energies of clusters in each silicon tungsten calorimeter was required to be less than 5 GeV. Furthermore the total cluster energy was required to be less than 2 GeV in each forward calorimeter and less than 5 GeV in each side of the gamma-catcher.

(A3) The magnitude of the cosine of the polar angle of the thrust axis, $|\cos\theta_{\rm thrust}|$, was required to be less than 0.95 in order to reduce the number of beam-gas and beam-wall background events as well as the events from two-photon processes.

case (A)	data	total bkg.	$\mathrm{q\bar{q}}(\gamma)$	$\ell\ell(\gamma)$	'$\gamma\gamma$'	4-f	$\mathrm{L}^0\bar{\mathrm{L}}^0$		
m_{L^0} (GeV)							60	70	70
Decay mode							tau	muon	electron
no cuts	–	–	1474	8428	220k	200	1000	1000	1000
cut (A1)	108k	56.0k	1433	105.6	54.4k	62.1	990	977	978
cut (A2)	36.5k	32.4k	1063	94.4	31.2k	47.7	867	883	853
cut (A3)	21.8k	19.2k	1028	91.0	18.0k	45.9	824	841	823
cut (A4)	1048	1062	923.8	82.7	10.9	44.2	793	837	818
cut (A5)	600	569.4	459.0	69.4	1.97	39.0	767	817	806
cut (A6)	114	102.5	82.6	0.50	0.18	19.2	681	767	752
cut (A7)	1	1.10	0.21	0.09	0.00	0.80	280	531	420
cut (A8)	0	0.54	0.14	0.04	0.00	0.36	272	467	381

Table 1: *The numbers of events remaining after each cut (in the* $\mathrm{L}^0\bar{\mathrm{L}}^0$ *search) are compared with various background processes, normalised to the integrated luminosity. Numbers are also given for three samples of simulated* $\mathrm{L}^0\bar{\mathrm{L}}^0$ *events.*

(A4) The visible energy, $E_{\rm vis}$, was required to be greater than $0.45\sqrt{s}$ to reduce the background from two-photon processes.

(A5) If the missing energy was larger than 30 GeV, the polar angle of the missing momentum direction, $\theta_{\rm miss}$, was required to satisfy $|\cos\theta_{\rm miss}| < 0.95$. One of the final states for the expected signals is $\ell\ell'{\rm qq'q''q'''}$, which has full visible energy. In this case the missing momentum direction is not meaningful, hence the missing energy threshold was applied.

(A6) The number of jets was required to be at least four. With this requirement a large fraction of the multihadron background was removed. The distributions of the number of jets after cut (A5) are shown in Fig. 1(a) for the data and the simulated background events, and in Fig. 1(b) for simulated $\rm L^0\bar{L}^0$ events.

(A7) The number of isolated leptons (e, μ or τ) was required to be at least two. The lepton identification and isolation requirements are the same as in Ref. [4], except that the upper bound on the momentum of one-prong tau decay was lowered from 40 GeV to 30 GeV. This cut is sensitive to all of light leptons (e, μ and τ) in the decay products of $\rm L^0$. The distributions of the number of isolated leptons after cut (A6) are plotted in Fig. 1(c) for the data and the simulated background events, and in Fig. 1(d) for simulated $\rm L^0\bar{L}^0$ events.

(A8) In order to reduce the $\ell^+\ell^-{\rm q\bar{q}}$ four-fermion background, the visible energy was required to be smaller than $0.85\sqrt{s}$ if the number of reconstructed jets was equal to four.

No event was observed in the data after the above selection. This result was consistent with the expected number of background events of 0.54. The detection efficiency for $\rm L^0\bar{L}^0$ events was calculated for various $m_{\rm L^0}$ values between 45 and 80 GeV. The efficiency for $m_{\rm L^0}$ in the range of 50–75 GeV was between 34% and 48% for $\rm L^0\bar{L}^0 \to eW^*eW^*$ or $\mu W^*\mu W^*$ events, and between 22% and 28% for $\rm L^0\bar{L}^0 \to \tau W^*\tau W^*$ events. For the mixed decay products of $\rm L^0\bar{L}^0$ ($\rm L^0\bar{L}^0 \to eW^*\mu W^*$, $\rm eW^*\tau W^*$ or $\rm \mu W^*\tau W^*$) the efficiencies have values intermediate to the unmixed cases. The efficiencies for the $\rm L^0\bar{L}^0 \to \tau W^*\tau W^*$ case were the lowest in this analysis.

3.2 Selection of $\rm L^+L^- \to \bar{\nu}_L W^{*+} \nu_L W^{*-}$ candidates (case B)

The numbers of events remaining after each cut are listed in Table 2 for case (B). For comparison the table also includes the corresponding numbers of simulated background and $\rm L^+L^-$ events. The reason for the difference in the number of events between the data and the simulated background before cut (B4) is the same as in case (A).

The following selection criteria were applied:

(B1) The number of charged tracks was required to be at least two, and the ratio of the number of tracks which satisfied the quality criteria to the total number of reconstructed tracks was required to be greater than 0.2.

(B2) The criteria for energy deposits in the silicon tungsten calorimeter, the forward calorimeter and the gamma-catcher were identical to those in the $\rm L^0\bar{L}^0$ analysis (see A2).

(B3) $|\cos\theta_{\rm thrust}|$ was required to be less than 0.9. The $|\cos\theta_{\rm thrust}|$ cut is harder than in the $\rm L^0$ analysis because the acoplanarity angle, which is discussed later, becomes unreliable if the jet axes are close to the beam direction.

(B4) Events from two-photon processes with a small visible energy were efficiently reduced by demanding that the event transverse momentum, P_t, calculated excluding the hadron calorimeter clusters to be larger than 4 GeV and the transverse momentum, $P_t^{\rm HCAL}$, calculated including the hadron calorimeter clusters to be larger than 5 GeV. Although most of the events from

two-photon processes were rejected by the P_t cut, the $P_t^{\rm HCAL}$ cut was applied to reject occasional events with a high transverse momentum neutral hadron. The distributions of the $P_t^{\rm HCAL}$ after cut (B3) are plotted in Fig. 2(a) for the data and the simulated background events and in Fig. 2(b) for simulated $\rm L^+L^-$ events.

case (B)	data	total bkg.	$\rm q\bar{q}(\gamma)$	$\ell\ell(\gamma)$	'$\gamma\gamma$'	4-f	$\rm L^+L^-$		
$m_{\rm L^-}$ (GeV)							70	70	65
$m_{\nu_{\rm L}}$ (GeV)							40	65	55
no cuts	–	–	1474	8428	220k	200	1000	1000	1000
cut (B1)	237k	101k	1436	1195	97.9k	83.0	981	934	968
cut (B2)	94.7k	66.6k	1063	1087	64.4k	59.1	944	915	933
cut (B3)	60.7k	37.2k	957.6	1010	35.2k	52.0	882	872	868
cut (B4)	1066	962.4	473.4	421.8	31.0	36.2	840	218	626
cut (B5)	356	344.8	170.1	140.3	11.3	23.1	630	208	520
cut (B6)	32	28.6	1.00	14.0	11.0	2.55	584	208	519
cut (B7)	18	18.7	0.83	11.0	5.29	1.60	521	136	371
cut (B8)	7	9.21	0.75	2.83	5.08	0.55	463	136	367
cut (B9)	2	1.48	0.40	0.29	0.58	0.21	412	118	304
cut (B10)	2	0.38	0.04	0.06	0.08	0.20	367	111	276

Table 2: *The numbers of events remaining after each cut (in the* $\rm L^- \to \nu_L W^{*-}$ *search) are compared with various background processes, normalised to the integrated luminosity. Expected numbers of events are also given for three samples of simulated* $\rm L^+L^-$ *events.*

(B5) The polar angle of the missing momentum direction $\theta_{\rm miss}$ should satisfy $|\cos\theta_{\rm miss}| < 0.7$. This reduces "Radiative return" events, in which initial state radiation results in an effective centre-of-mass energy near the $\rm Z^0$ resonance, and two-photon events.

(B6) A visible energy cut was applied to reduce both multihadron and four-fermion background. The visible energy of $\rm L^+L^-$ events was expected to be smaller than about 80 GeV, since the two heavy $\nu_{\rm L}$'s carry away a significant fraction of the energy. The visible energy was thus required to be smaller than $0.45\sqrt{s}$.

(B7) In order to reduce the remaining events from two-photon processes two requirements were adopted: $E(|\cos\theta|{>}0.8)/E_{\rm vis} < 1.5\ E_{\rm vis}/\sqrt{s}$ and $|P_z| < 0.4\ E_{\rm vis}$, where $E(|\cos\theta|{>}0.8)$ is the visible energy in the region of $|\cos\theta| > 0.8$ and P_z is the missing momentum along the beam direction.

(B8) Background from $\tau^+\tau^-(\gamma)$ and four-fermion processes was reduced by requiring that no track momentum exceed 20 GeV.

(B9) In order to reject events containing two back-to-back jets or leptons, the thrust of the event was required to be less than 0.9.

(B10) The acoplanarity angle[4] ($\phi_{\rm acop}$) between the two thrust hemisphere momenta was required to be greater than 15°. If all the visible decay products of $\rm L^-$ and $\rm L^+$ happened to be in the

[4] $\phi_{\rm acop}$ was defined as $\pi - \phi_{\rm open}$, where $\phi_{\rm open}$ is the azimuthal opening angle between the directions of the momentum sums of the particles in the two thrust hemispheres.

same hemisphere, the event topology could be a monojet and $\phi_{\rm acop}$ was defined to be 180°. The acoplanarity angle distributions just before the cut are shown in Fig. 2(c) for the data and the simulated background events, and in Fig. 2(d) for simulated L^+L^- events.

Two candidate events were observed in the data after the above selection. The visible energy of one of the two candidate events was 55 GeV, and the missing momentum was 39 GeV. The event topology of this candidate event was consistent with the $ZZ^* \to \nu\bar{\nu}q\bar{q}$ process. This event was also selected as a candidate event in the searches for chargino/neutralino and scalar top/bottom quark [19]. The other candidate is shown in Fig. 3. This event could be interpreted as $Z\gamma^* \to \tau\tau\phi$, with ϕ decaying into $K^0_L K^0_S$. The expected number of background events from all sources was estimated to be 0.38.

The efficiency of this selection was about 11% for (m_{L^-}, m_{ν_L}) = (70 GeV, 65 GeV) and 36% for (70 GeV, 40 GeV).

3.3 Selection of $L^+L^- \to \bar{\nu}_\ell W^{*+} \nu_\ell W^{*-}$ candidates (case C)

The numbers of events remaining after each cut are listed in Table 3 for case (C). For comparison the table also includes the corresponding numbers of simulated background and L^+L^- events. The reason for the difference in the number of events between the data and the simulated background before cut (C3) is the same as in case (A).

The following selection criteria were applied:

(C1) The number of tracks was required to be at least five, and the ratio of the number of tracks which satisfied the quality criteria to the total number of reconstructed tracks was required to be larger than 0.2 in order to reject beam-gas and beam-wall backgrounds.

(C2) The criteria for energy deposits in the silicon tungsten calorimeter, the forward calorimeter and the gamma-catcher were identical to those in the $L^0\bar{L}^0$ analysis (see A2).

(C3) $|\cos\theta_{\rm thrust}|$ was required to be less than 0.95 in order to reduce beam-gas and beam-wall background events as well as events from two-photon processes.

(C4) The transverse momentum was expected to be large for the L^+L^- signal events, hence P_t and $P_t^{\rm HCAL}$ were required to be larger than 12 GeV and 15 GeV, respectively. With this cut the background from two-photon processes was efficiently reduced.

(C5) "Radiative return" events were rejected by requiring that the $\theta_{\rm miss}$ should satisfy $|\cos\theta_{\rm miss}| < 0.9$. The $|\cos\theta_{\rm miss}|$ cut was looser than in case (B) because the P_t and $P_t^{\rm HCAL}$ cuts in case (C) were tighter than in case (B).

(C6) In order to reject events containing two back-to-back jets or leptons, the thrust of the event was required to be less than 0.9.

The remaining events were classified into two categories, HL and HH, using the same lepton identification as in the $L^0\bar{L}^0$ case [4]. The expected final states are $L^+L^- \to \bar{\nu}_\ell W^{*-} \nu_\ell W^{*+} \to \nu_\ell \ell' \nu_{\ell'} \nu_\ell qq'$, $\nu_\ell qq' \nu_\ell q'' q'''$ or $\nu_\ell \ell' \nu'_\ell \nu_\ell \ell'' \nu_{\ell''}$.

- (HL) If there were three reconstructed jets, including one lepton (e, μ or τ) with a momentum larger than 8 GeV, the event was classified as (HL) event, corresponding to the $\nu_\ell \ell' \nu_{\ell'} \nu_\ell qq'$ final states.

case (C)	data	total bkg.	$q\bar{q}(\gamma)$	$\ell\ell(\gamma)$	'$\gamma\gamma$'	4-f	L^+L^-	
m_{L^-} (GeV)							65	75
no cuts	–	–	1474	8428	220k	200	1000	1000
cut (C1)	75.4k	43.6k	1431	24.8	42.1k	59.9	900	914
cut (C2)	24.6k	23.8k	1063	21.9	22.7k	46.3	826	869
cut (C3)	13.6k	13.3k	1028	17.3	12.2k	44.6	793	831
cut (C4)	124	112.1	90.5	4.76	2.06	14.8	609	645
cut (C5)	85	88.4	69.2	4.22	0.79	14.2	589	631
cut (C6)	38	34.6	23.2	0.81	0.23	10.4	535	544
(HL)	3	6.57	2.31	0.24	0.00	4.02	173	192
cut (HL7)	0	0.56	0.28	0.07	0.00	0.21	122	133
cut (HL8)	0	0.23	0.00	0.03	0.00	0.20	111	120
(HH)	8	5.65	4.20	0.00	0.08	1.37	157	179
cut (HH9)	4	2.38	1.72	0.00	0.00	0.66	146	165
cut (HH10)	3	1.56	0.91	0.00	0.00	0.65	144	159
cut (HH11)	2	1.19	0.68	0.00	0.00	0.51	134	144
cut (HH12)	0	0.43	0.10	0.00	0.00	0.33	108	114
(HL8)+(HH11)	0	0.66	0.10	0.03	0.00	0.53	219	234

Table 3: *The numbers of events remaining after each cut (in the* $L^- \to \nu_\ell W^{*-}$ *search) are compared with various background processes, normalised to the integrated luminosity. Expected numbers of events are also given for two samples of simulated* L^+L^- *events.*

- (HH) If there was no track identified as a lepton with a momentum larger than 8 GeV and if the number of jets was equal to four, the event was categorized as (HH) event, corresponding to the $\nu_\ell q q' \nu_\ell q'' q'''$ final states.

The events which were not classified as (HL) or (HH) events were rejected in order to reduce the multihadron and four-fermion background.

(HL7) For (HL) events the visible energy was required to satisfy $0.25\sqrt{s} < E_{\rm vis} < 0.6\sqrt{s}$. With this cut background from four-fermion processes and multihadron events were effectively reduced.

(HL8) The acoplanarity angle ($\phi_{\rm acop}$) was required to be greater than 10° to reject multihadron events.

(HH9) For (HH) events the visible energy was required to satisfy $0.4\sqrt{s} < E_{\rm vis} < 0.9\sqrt{s}$. Multihadron background was reduced by this cut.

(HH10) The remaining background comes primarily from hadronic events in which a mismeasurement of the energy of a jet leads to an artificial missing momentum. This missing momentum tends to lie along the jet directions in ordinary multihadron events. We defined the total energy sum, $E_{\rm back}$, within a cone of 20° half-angle around the direction of the missing momentum. $E_{\rm back}$ was required to be less than 5 GeV in order to reduce a large fraction of the multihadron background.

(HH11) Four-fermion processes and multihadron events were reduced by requiring that no track momentum should exceed 30 GeV.

(HH12) The acoplanarity angle ($\phi_{\rm acop}$) was required to be greater than 15° to reject multihadron events. The acoplanarity angle distributions just before the cut are plotted in Fig. 2(e) for the data and the simulated background events and in Fig. 2(f) for simulated L^+L^- events.

The detection efficiency was about 20–24% for m_{L^-} in the range 60–80 GeV. No event was observed in the data after the above selection, consistent with the total of 0.66 background events expected.

4 Mass Limits

The expected numbers of neutral and charged heavy lepton events were estimated for various values of the heavy lepton mass (or combinations of (m_{L^-}, m_{ν_L})) using the detection efficiency, the cross-section and the integrated luminosity. In calculating mass limits the detection efficiency at an arbitrary value of the heavy lepton mass was interpolated using a polynomial fit between the simulated mass points.

The systematic errors on the total number of expected signal events were estimated to be 3–6% from Monte Carlo statistics, depending on the event topology, 0.2% (1.0%) from the uncertainty on the beam energy for $L^0\bar{L}^0$ (L^+L^-), 1.3% from the uncertainty due to the detector simulation, 1.0% from the interpolation of the efficiencies, 0.6% from the uncertainty in the integrated luminosity, 3.5% from the lepton identification uncertainty, and 1.6% (0.9%) from the uncertainty in the fragmentation of W^* hadronic decays for $L^0\bar{L}^0$ (L^+L^-). The fragmentation errors arose through the jet reconstruction and lepton isolation uncertainties for the $L^0\bar{L}^0$ case, and mainly through the uncertainty in the estimation of the acoplanarity angle and the missing momentum direction for the L^+L^- case. The fragmentation error was estimated by varying the fragmentation parameters from their optimized values [20] in the JETSET 7.4 Monte Carlo generator. The systematic error due to trigger efficiency was estimated to be negligible for the selected signal events. The individual systematic errors were considered to be independent, and the total systematic error was calculated as their quadratic sum. In calculating mass limits the systematic errors were treated as described in Ref. [21].

Lower mass limits for L^0 were calculated by combining the number of expected events in this analysis with those from the analysis at $\sqrt{s}$ = 130 and 136 GeV [4]. A 95% C.L. lower limit of 69.3 GeV is obtained on the mass of the Dirac neutral heavy lepton, assuming that both L^0 and $\bar{L}^0$ decay into eW^* with 100% branching fraction. Corresponding limits for the cases of $L^0 \to \mu W^*$ and $L^0 \to \tau W^*$ are 72.0 GeV and 66.0 GeV, respectively. For the Majorana L^0 the limits are reduced due to the smaller cross-section near the $L^0\bar{L}^0$ threshold to 59.5 GeV for the eW^* decay, 60.5 GeV for the μW^* decay and 55.7 GeV for the τW^* decay due to the smaller cross-section near the $L^0\bar{L}^0$ threshold. For the mixed decay products of $L^0\bar{L}^0$ ($L^0\bar{L}^0 \to eW^*\mu W^*$, $eW^*\tau W^*$ or $\mu W^*\tau W^*$) the mass limits have values intermediate to the unmixed cases.

The mass of the $L^\pm$ was found to be larger than 73.5 GeV at 95% C.L. for case (B), if m_{L^-} - $m_{\nu_L} > 13$ GeV. In calculating the mass limits, the two candidate events observed were considered as possible signals and the expected number of background events was not subtracted. The excluded region in the (m_{L^-}, m_{ν_L}) plane for case (B) is presented in Fig. 4. For case (C) the lower limit for m_{L^-} is 76.7 GeV at 95% C.L.

5 Summary and Conclusions

A search has been made for pair production of unstable neutral and charged heavy leptons using a data sample corresponding to an integrated luminosity of 10.0 pb^{-1} at $\sqrt{s} = 161.3$ GeV, collected with the OPAL detector at LEP. No event remained after the selection cuts for the $\mathrm{L}^0\bar{\mathrm{L}}^0$ and $\mathrm{L}^- \to \nu_\ell \mathrm{W}^{*-}$ searches. For the $\mathrm{L}^- \to \nu_\mathrm{L} \mathrm{W}^{*-}$ search, two candidate events were observed. These results were consistent with the expected total number of background events of 1.57.

The 95% C.L. lower limit on the Dirac L^0 mass, assuming that L^0 decays into eW^* with 100% branching fraction, was determined to be 69.3 GeV. The mass limits for $\mu\mathrm{W}^*$ and $\tau\mathrm{W}^*$ decays are 72.0 GeV and 66.0 GeV, respectively. For the Majorana L^0 the limits were reduced due to the smaller cross-section near the $\mathrm{L}^0\bar{\mathrm{L}}^0$ threshold to 59.5 GeV for pure eW^* decay, 60.5 GeV for pure $\mu\mathrm{W}^*$ decay and 55.7 GeV for the $\tau\mathrm{W}^*$ case.

The excluded region in the $(m_{\mathrm{L}^-}, m_{\nu_\mathrm{L}})$ plane is presented in Fig. 4. If $m_{\mathrm{L}^-} - m_{\nu_\mathrm{L}} > 13$ GeV, the mass of the L^- was found to be larger than 73.5 GeV at 95% C.L. If $m_{\nu_\mathrm{L}} > m_{\mathrm{L}^-}$ and the L^- decays into a massless neutrino and a virtual W boson, a lower limit of 76.7 GeV at 95% C.L. was obtained for m_{L^-}. The results of these analyses have extended existing limits from the LEP experiments [2, 3, 4].

6 Acknowledgements

We particularly wish to thank the SL Division for the efficient operation of the LEP accelerator at the new energy of $\sqrt{s} = 161$ GeV and for their continuing close cooperation with our experimental group. We thank our colleagues from CEA, DAPNIA/SPP, CE-Saclay for their efforts over the years on the time-of-flight and trigger systems which we continue to use. We also thank Francesca Borzumati of the Weizmann Institute for her strong theoretical support. In addition to the support staff at our own institutions we are pleased to acknowledge the
Department of Energy, USA,
National Science Foundation, USA,
Research Corporation, USA,
Particle Physics and Astronomy Research Council, UK,
Natural Sciences and Engineering Research Council, Canada,
Israel Science Foundation, administered by the Israel Academy of Science and Humanities,
Minerva Gesellschaft,
Japanese Ministry of Education, Science and Culture (the Monbusho) and a grant under the Monbusho International Science Research Program,
German Israeli Bi-national Science Foundation (GIF),
Bundesministerium für Bildung, Wissenschaft, Forschung und Technologie, Germany,
National Research Council of Canada,
Hungarian Foundation for Scientific Research, OTKA T-016660, and OTKA F-015089.

References

[1] L. Montanet *et al.*, Phys. Rev. D50 (1994) 1418.

[2] ALEPH Collab., D. Decamp *et al.*, Phys. Lett. B236 (1990) 511;
OPAL Collab., M.Z. Akrawy *et al.*, Phys. Lett. B240 (1990) 250;
OPAL Collab., M.Z. Akrawy *et al.*, Phys. Lett. B247 (1990) 448;
L3 Collab., B. Adeva *et al.*, Phys. Lett. B251 (1990) 321;
OPAL Collab., G. Alexander *et al.*, Z. Phys. C52 (1991) 175;
DELPHI Collab., P. Abreu *et al.*, Phys. Lett. B274 (1992) 230.

[3] L3 Collab., M. Acciarri *et al.*, "Search for Unstable Sequential Neutral and Charged Heavy Leptons in e^+e^- Annihilation at $\sqrt{s}$ = 130 and 136 GeV", CERN-PPE/96-038 (1996), to be published in Phys. Lett. B.;
ALEPH Collab., D. Buskulic *et al.*, "Search for heavy lepton pair production in e^+e^- collisions at centre-of-mass energies of 130 and 136 GeV", CERN-PPE/96-080 (1996), submitted to Phys. Lett B.

[4] OPAL Collab., G. Alexander *et al.*, "Search for Unstable Neutral and Charged Heavy Leptons in e^+e^- Collisions at $\sqrt{s}$ = 130 and 136 GeV", CERN-PPE/96-093 (1996), to be published in Phys. Lett. B.

[5] H. Baer *et al.*, in "Physics at LEP", vol. 1, eds. J. Ellis and R. Peccei, CERN 86-02 (1986) 297.

[6] OPAL Collab., K. Ahmet *et al.*, Nucl. Instr. Meth. A305 (1991) 275;
P. P. Allport *et al.*, Nucl. Instr. Meth. A324 (1993) 34;
P. P. Allport *et al.*, Nucl. Instr. Meth. A346 (1994) 476;
B.E. Anderson *et al.*, IEEE Trans. Nucl. Sci. 41 (1994) 845.

[7] S. Jadach and J. Kühn, preprint MPI-PAE/PTh 64/86.

[8] T. Sjöstrand, Comp. Phys. Comm. 82 (1994) 74.

[9] F.A. Berends, R. Kleiss and S. Jadach, Nucl. Phys. B202 (1982) 63;
F.A. Berends, R. Kleiss and S. Jadach, Comp. Phys. Comm. 29 (1983) 185.

[10] S. Jadach, B. F. L. Ward and Z. Wąs, Comp. Phys. Comm. 79 (1994) 503.

[11] S. Jadach, W. Płaczek and B. F. L. Ward, University of Tenessee preprint UTHEP-95-1001 (unpublished);
S. Jadach, W. Płaczek and B. F. L. Ward, in "Physics at LEP2", eds. G. Altarelli, T. Sjöstrand and F. Zwirner, CERN 96-01, vol. 2 (1996) 229.

[12] R. Engel, Z. Phys. C66 (1995) 203.

[13] G. Marchesini *et al.*, Comp. Phys. Comm. 67 (1992) 465.

[14] J. A. M. Vermaseren, Nucl. Phys. B229 (1983) 347.

[15] F.A Berends, R. Pittau and R. Kleiss, Comp. Phys. Comm. 85 (1995) 437.

[16] J. Allison *et al.*, Nucl. Instr. Meth. A317 (1992) 47.

[17] OPAL Collab., G. Alexander *et al.*, Phys. Lett. B377 (1996) 181;
OPAL Collab., G. Alexander *et al.*, Phys. Lett. B377 (1996) 273.

[18] N. Brown and W.J. Stirling, Phys. Lett. B252 (1990) 657;
S. Catani *et al.*, Nucl. Phys. B269 (1991) 432;
S. Bethke, Z. Kunszt, D. Soper and W.J. Stirling, Nucl. Phys. B370 (1992) 310;
N. Brown and W.J. Stirling, Z. Phys. C53 (1992) 629.

[19] OPAL Collab., G. Alexander *et al.*, "Search for Chargino and Neutralino Production at $\sqrt{s} = 161$ GeV", CERN-PPE/96-135 (1996), submitted to Phys. Lett. B;
OPAL Collab., G. Alexander *et al.*, "Search for scalar top and scalar bottom quarks using the OPAL detector at LEP ", CERN-PPE/96-133 (1996), submitted to Phys. Lett. B.

[20] OPAL Collab., G. Alexander *et al.*, Z. Phys. C69 (1996) 543.

[21] R.D. Cousins and V.L. Highland, Nucl. Instr. Meth. A320 (1992) 331.

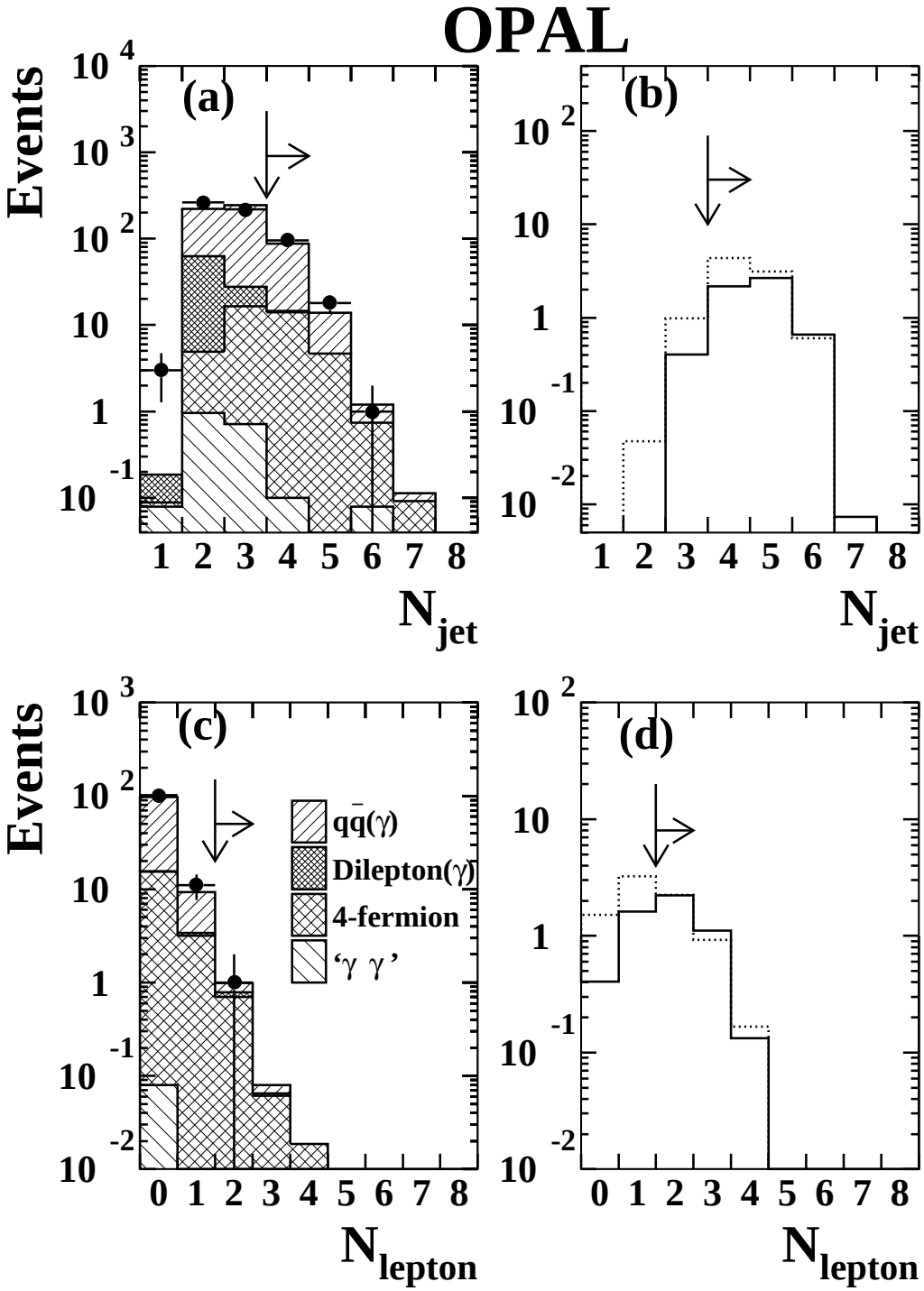

Figure 1: The distributions of the number of jets before cut (A6) for the data (bold circles with error bars) and for the simulated background events are plotted in (a). The same distributions are shown in (b) for simulated $L^0\bar{L}^0 \to eW^*eW^*$ events with $m_{L^0} = 70$ GeV (solid line histogram) and $L^0\bar{L}^0 \to \tau W^*\tau W^*$ events with $m_{L^0} = 60$ GeV (dotted line histogram). The arrows indicate the position of the cut and the region accepted. The distributions of the number of isolated leptons before cut (A7) for the data and the simulated background events are displayed in (c). The distributions of the number of isolated leptons for the $L^0\bar{L}^0$ events are shown in (d) for the same samples as in (b).

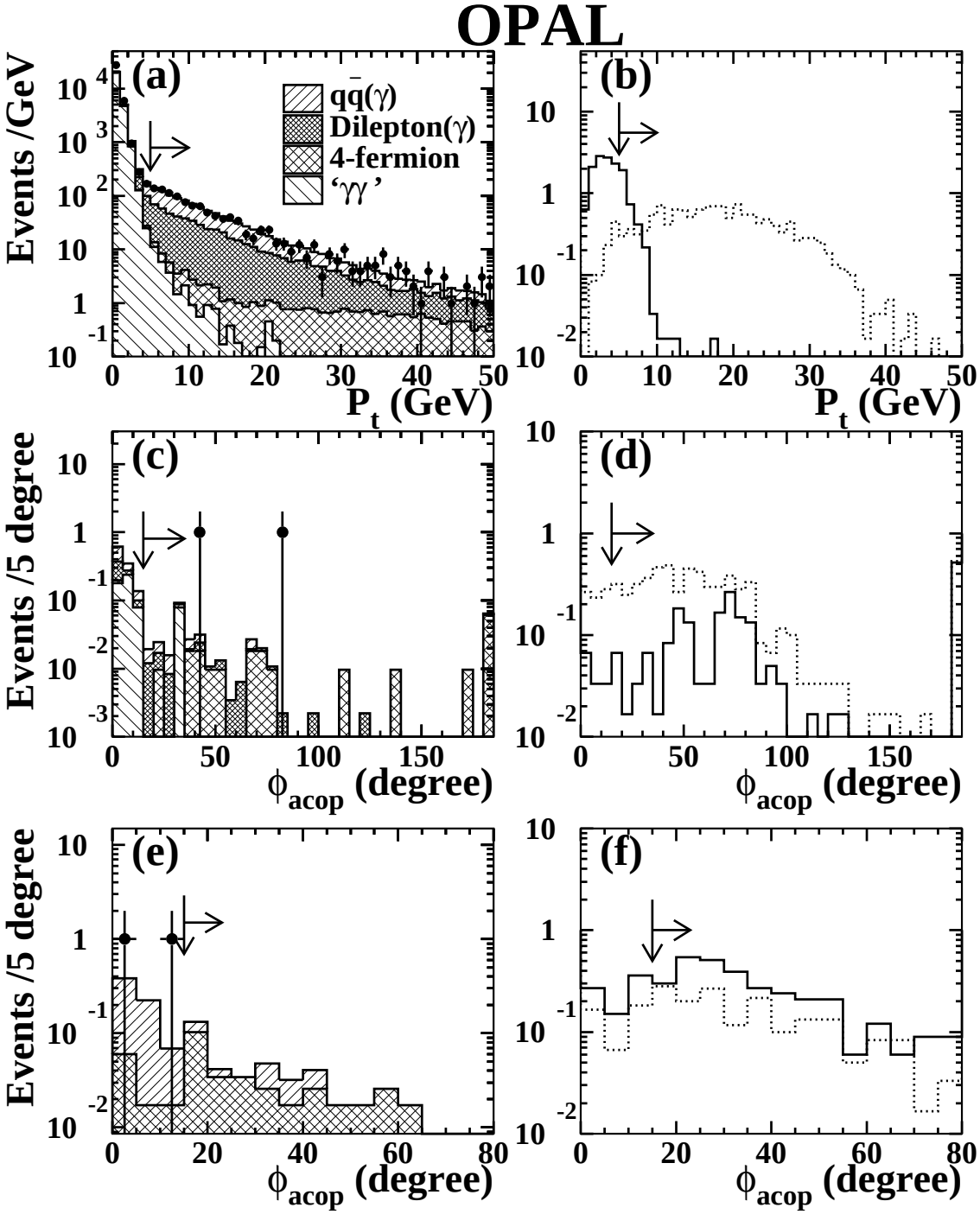

Figure 2: The missing transverse momentum, $P_t^{\rm HCAL}$, distributions before cut (B4) for the data (bold circles with error bars) and for the simulated background events are plotted in (a). The same distributions are shown in (b) for simulated $\mathrm{L}^- \to \nu_{\mathrm{L}}\mathrm{W}^{*-}$ events with $(m_{\mathrm{L}^-}, m_{\nu_{\mathrm{L}}}) = (70,\ 65)$ GeV (solid line histogram) and $(m_{\mathrm{L}^-}, m_{\nu_{\mathrm{L}}}) = (70,\ 40)$ GeV (dotted line histogram). The arrows indicate the position of the cut and the region accepted. Acoplanarity angle distributions plotted for data (bold circles with error bars) and various simulated background processes before cut (B10) for case (B) or (HH12) for case (C) are shown in (c) and (e), respectively. The distributions of the acoplanarity angle for case (B) are shown in (d) for the same samples as in (b). In (f) the solid and dotted histograms represent simulated $\mathrm{L}^+\mathrm{L}^-$ events with $\mathrm{L}^- \to \nu_\ell \mathrm{W}^{*-}$ decay for $m_{\mathrm{L}^-} = 65$ GeV and 75 GeV, respectively.

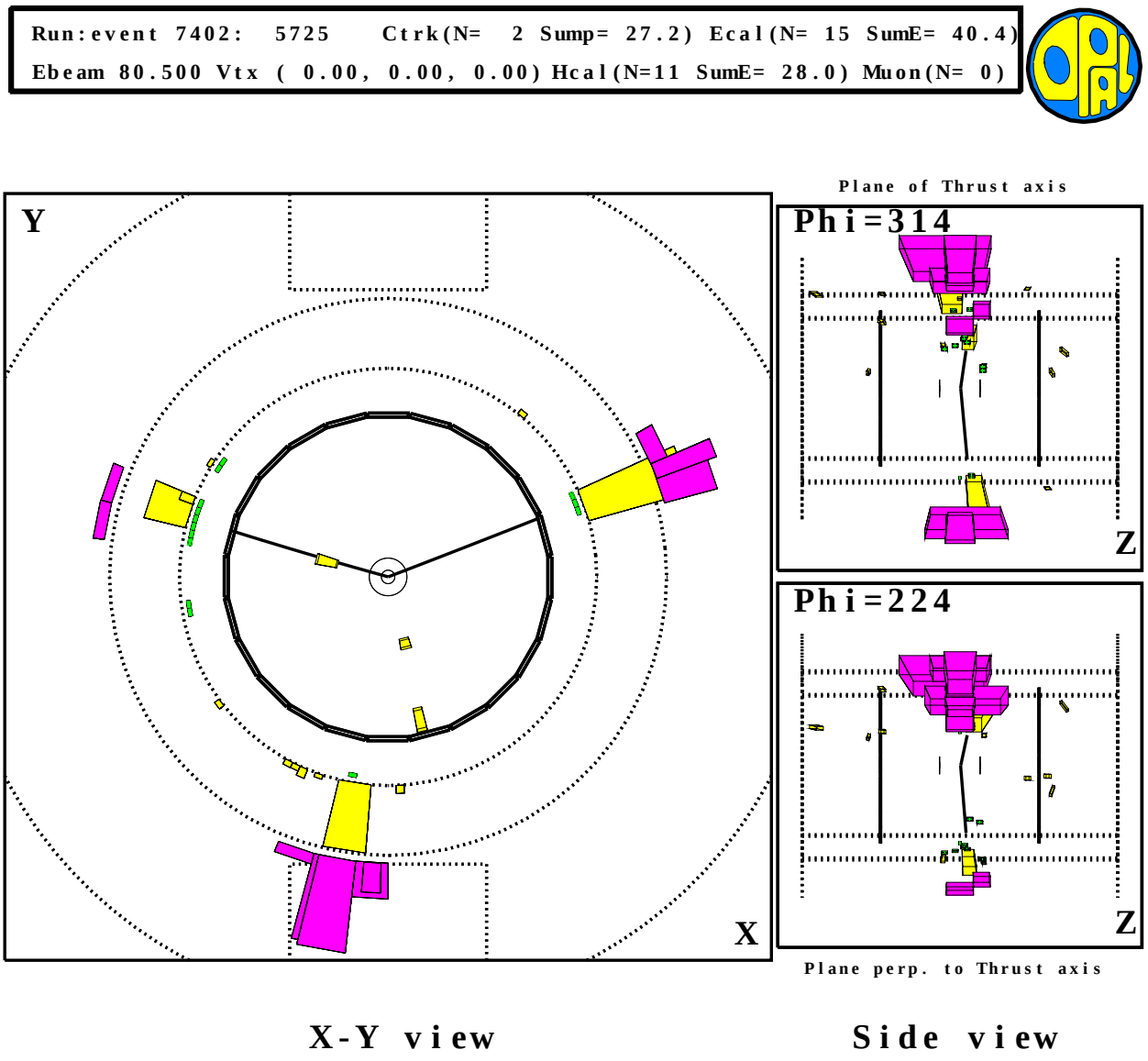

Figure 3: One of the two candidate events for case (B). The visible energy of the event is 71 GeV, and the missing transverse momentum is 23 GeV. The dark lines represent fitted charged tracks in the tracking chambers. The light grey boxes indicate the relative energies deposited in EM clusters. The dark grey boxes indicate the relative amount of energies deposited in HCAL clusters.

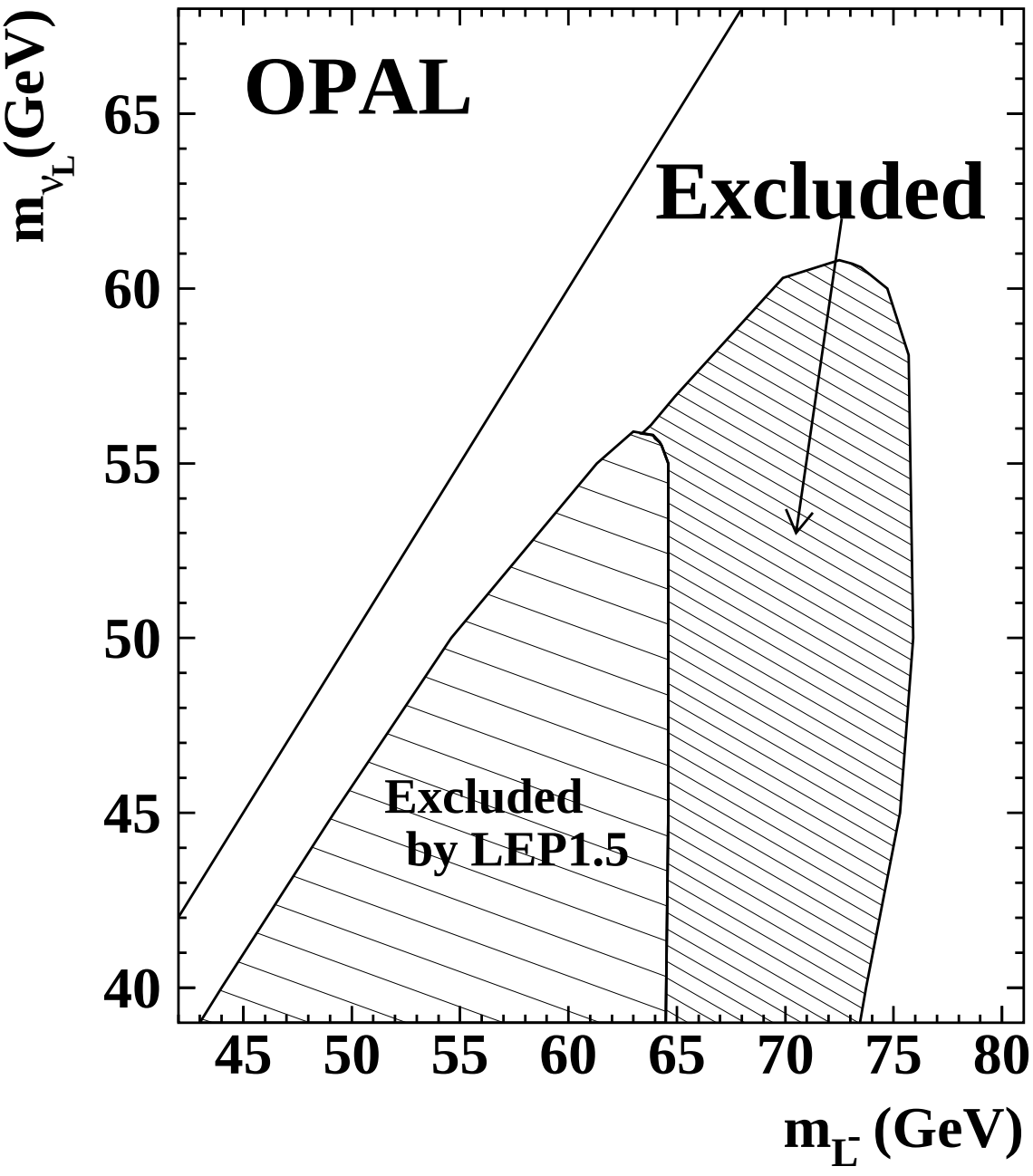

Figure 4: The region excluded in this analysis in the (m_{L^-}, m_{ν_L}) plane for case (B). If L^- decays into $\nu_\mathrm{L} + \mathrm{W}^{*-}$ and ν_L is assumed to be stable, the hatched region is excluded with more than 95% C.L. The region $m_{\nu_\mathrm{L}} < 45.0$ GeV is already excluded for the Dirac ν_L and $m_{\nu_\mathrm{L}} < 39.5$ GeV for the Majorana ν_L at LEP1 [1, 2]. The diagonal line shows $m_{\mathrm{L}^-} = m_{\nu_\mathrm{L}}$.